11th World Congress on Structural and Multidisciplinary Optimisation
07th -12th, June 2015, Sydney Australia

Stability-ensured topology optimization of boom structures with stress constraints

Wenjun Li[1], Qicai Zhou[1], Zhen Jiang[2], Wei Chen[2]

[1] Tongji University, Shanghai, China, wenjun.li.nu@gmail.com, qczhou@tongji.edu.cn
[2] Northwestern University, Evanston, USA, ZhenJiang2015@u.northwestern.edu, weichen@northwestern.edu

1. Abstract

The use of giant boom cranes has gained an ever-increasing popularity due to their superior handling abilities. Lightweight design of a giant boom structure, which is usually achieved by topology optimization, becomes critical in reducing the energy consumption of the whole crane. In topology optimization of giant boom structures, geometrically nonlinear analysis has been adopted to capture the accurate structural response. A common issue is that the stiffness of some members keeps decreasing during the optimization process, which is often a generator of some slender struts leading to buckling issue. Therefore, a stability-ensured topology optimization algorithm for structural design is needed to maintain sufficient stability of boom structures while reducing the weight.

The stability performance is studied either as a constraint or as an objective in topology optimization problems [1]. The evolutionary structural optimization (ESO) method was extended to linear buckling problems, and a simple method not involving variational calculus or Lagrangian multipliers was presented for the optimum design of columns and frames [2]. Kemmler et al. [3] considered the lowest critical load level as an inequality constraint and conducted topology optimization of structures including kinematics. The design problem of maximizing the buckling load factor of laminated composite shell structures was investigated using the discrete material optimization approach [4-6]. Lindgaard and Dahl [7] investigated a range of different compliance and buckling objective functions for maximizing the buckling resistance of a snap-through beam structure. The gradient-based optimization methods have been widely applied in many stability constrained problems, but they are not appropriate for topology optimization problems with large number of local stability constraints due to difficulties in calculating the sensitivities of numerous constraints with respect to each of the design variables.

In the presence of aforementioned drawbacks of gradient-based methods, non-gradient-based methods are put forward to provide a convenient way for topology optimization of geometrically nonlinear boom structures. Although non-gradient nature-inspired methods are not viable alternatives for the vast majority of topology optimization problems, they actually solve discrete topology optimization problems with surprisingly high efficiency [8]. For example, the Soft Kill Option (SKO) method is a heuristic topology optimization method based on the simulation of the biological growth rule of biological growth carriers like bones [9]. It reduces human error to a minimum, and even in really complex cases makes it possible for the first time to find a draft design that is already close to the optimum [10]. Even though sensitivity analysis is not used, the results obtained with the SKO method are very similar to those by gradient-based methods using OptiStruct [11, 12]. Our previous work [13] extended the SKO method into topology optimization of bars structures and sets the foundation for this research.

A couple of member buckling judgment methods for bars structures have been presented in recent years. Shen et al. [14] proposed a middle plastic hinge model of the member, assuming that the member is in a completely elastic deformation condition before buckling. Fan et al. [15] adopted the curve of axial force-relative deflection of the member and the energy method to judge the member buckling. To better monitor the stability of the structure, global stability index (GSI) and compression member stability index (MSI) are defined in this paper. The global stability constraint can be easily formulated by GSI, while member buckling of any compression member can be detected by MSI. Apart from stability, the volume and stress should also be taken into consideration in topology optimization of boom structures so that the topology design is close to industrial application. However, it is very difficult to find optimization algorithms for discrete problems that can treat multiple non-trivial constraints [8]. The traditional volume constraint always conflicts with global stability and stress constraints, thus the predetermined target volume fraction may not be achieved. Adaptive volume constraint algorithm is proposed by Lin and Sheu [16] so that the maximum stress in the optimal structural configuration is guaranteed to be below the predefined stress limit.

The stability indices are utilized as a part of a novel Stability-Ensured Soft Kill Option (SSKO) algorithm, which is a heuristic topology optimization approach proposed in this work on the basis of the existing SKO method. The objective is to minimize the discrepancy between structural volume and predetermined target volume, while the global stability, member stability and stress are regarded as constraints. To demonstrate the effectiveness of the proposed approach, the SSKO algorithm with different scenarios is applied to topology optimization of a ring crane boom, and stable topologies are achieved with high efficiency and consistency.

2. Keywords: boom structures, topology optimization, stability index, Stability-Ensured Soft Kill Option, geometric nonlinearity

3. Stability indices

3.1. Global stability index

For a static structure, the overall stiffness can be defined as the slope of load-displacement curve of a certain position at the last convergence incremental step, represented by S_g. A positive S_g infers a stable structure, while S_g decreases to zero or a negative number when the structure becomes global buckling. In the process of topology optimization, we need to quantitatively express the global stability status for monitoring the global stability constraint, and the global stability index (GSI) is defined as

$$GSI^{(k)} = S_g^{(k)} / S_g^{(0)},\ k = 0,1,...,k_{\max} \tag{1}$$

where k is the indicator of iteration number, k=0 means the initial analysis of the structure, and $k_{\max}$ is the maximum number of iterations. $GSI^{(k)}$ is the global stability index in the k-th iteration, and $S_g^{(k)}$ denotes the overall stiffness of the structure in the k-th iteration. $GSI^{(0)}$ is equal to 1 if the whole structure is stable in the initial analysis. Similar to the overall stiffness, a positive GSI infers a stable structure, while it decreases to zero or a negative number when the structure becomes global buckling.

3.2. Compression member stability index

Fig.1 shows the deformation of a compression member in the global coordinate system O-XYZ. AB is the initial configuration before deformation and $A'B'$ is the configuration after deformation. All the non-end loads have been converted to the end loads, such as gravity load and wind load. Two local coordinate systems, the member coordinate system A'-xyz and the member end coordinate system B'-$x_o y_o z_o$, are defined as follows. In the member coordinate system: the direction of vector $\overrightarrow{A'B'}$ (pointing from A' to B') is defined as $+x$ direction, $+y$ direction is parallel to plane XY and its angle with $+Y$ is smaller than or equal to 90°; in the case when axial x is parallel to axial Z, axial y is defined to be parallel to axial Y. In the member end coordinate system, the outward tangential direction at B' is defined as $+x_o$ direction, $+y_o$ direction is parallel to plane XY and its angle with $+Y$ is smaller than or equal to 90°; similarly to the member coordinate system, when axial x_o is parallel to axial Z, axial y_o is defined to be parallel to axial Y. Both local coordinate systems are right-handed and depend on the configuration after deformation. The loading condition at the end B' is expressed in the member end coordinate system (Fig.1). They are three force components $\boldsymbol{F}_{x_o}$, $\boldsymbol{F}_{y_o}$, $\boldsymbol{F}_{z_o}$ and three bending moments $\boldsymbol{M}_{x_o}, \boldsymbol{M}_{y_o}, \boldsymbol{M}_{z_o}$.

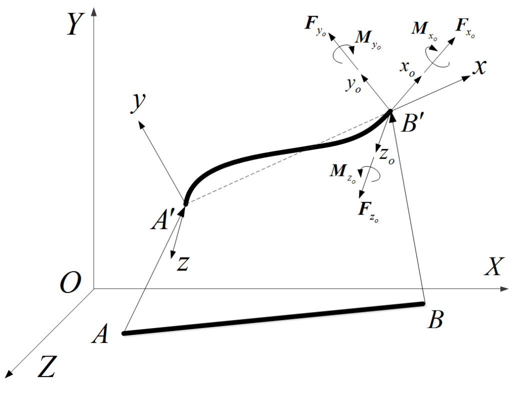

Figure 1: Deformation of a compression member

The axial vector of member AB after deformation is

$$\boldsymbol{a} = A'B' \tag{2}$$

The three force components $\boldsymbol{F}_{x_o}, \boldsymbol{F}_{y_o}, \boldsymbol{F}_{z_o}$ are projected onto the axial vector, and the projection sum is the axial force of member AB after deformation

$$F_a = (\boldsymbol{F}_{x_o} + \boldsymbol{F}_{y_o} + \boldsymbol{F}_{z_o}) \cdot \boldsymbol{a} / \|\boldsymbol{a}\| \tag{3}$$

where $\| \ \|$ denotes the module of a vector, similarly hereinafter; a positive value of F_a means tension while a negative value means compression.

The relative axial displacement between the ends of member AB is written as

$$\Delta u = \|\boldsymbol{a}\| - \|AB\| \tag{4}$$

A positive value of Δu means elongation while a negative value means shortening.

For any member AB in a frame structure, its axial stiffness at time t can be defined as

$$^{t}S_a = (^{t}F_a - {}^{t-\Delta t}F_a)/(^{t}\Delta u - {}^{t-\Delta t}\Delta u) \tag{5}$$

Here $t-\Delta t$ is the time with a tiny time period Δt difference prior to time t.

According to the definition of stability of compression members, when the axial compression force begins to decline and the absolute value of the relative axial displacement is still increasing, this member is buckling. In other words, a compression member is buckling when its $^{t}S_a$ value changes from a positive number to a negative number. Hence, capturing the changes of axial stiffness can help judge whether a compression member is unstable. This judgment method is applicable to the elastic or elastoplastic, limit point, flexural or flexural-torsional buckling of compression member considering only the end forces.

In the optimization process, we can quantitatively evaluate the compression member stability status by thee MSI defined as

$$MSI_{(j)}^{(k)} = S_{a(j)}^{(k)} / S_{a(j)}^{(0)},\ k = 0,1,...,k_{\max} \tag{6}$$

where $MSI_{(j)}^{(k)}$ is the stability index of member *j* in the *k*-th iteration. $S_{a(j)}^{(k)}$ denotes the axial stiffness of member *j* in the *k*-th iteration, which is determined in Eq. (5). is equal to 1 if member *j* is stable in the initial analysis. When $MSI_{(j)}^{(k)}$ decreases to zero or a negative value, the compression member *j* buckles.

4. Optimization procedure

4.1. Formulation of the optimization problem

The stability-ensured topology optimization of boom structures with volume and stress considerations can be formulated as follows:

$$\begin{aligned}
&\text{find} && \boldsymbol{E} = (E_1, E_2, \quad, E_n)^{\mathrm{T}} \\
&\min && \left| \sum_{j=1}^{n} (v_{oj} E_j / E_{\max}) - V_o \times vf_{\text{target}} \right| \quad (j = 1,2, \quad, n) \\
&\text{s.t.} && GSI > 0 \\
& && MSI_{(j)} > 0 \qquad (j = 1,2, \quad, n) \\
& && \sigma_{\max} \le [\sigma] \\
& && E_{\min} \le E_j \le E_{\max} \qquad (j = 1,2, \quad, n)
\end{aligned} \tag{7}$$

Where E_j is the Young's modulus of member j $(j = 1,2, \quad, n)$, v_{oj} is the initial volume of member j, $\sum_{j=1}^{n}(v_{oj}E_j/E_{\max})$ denotes the total volume of design domain, V_o is the total volume of initial structure in a design domain and vf_{target} is the predetermined target volume fraction. GSI is the global stability index defined in Eq. (1), $\sigma_{\max}$ is the maximum stress, and $[\sigma]$ is the allowable stress. $E_{\min}$ and $E_{\max}$ are the lower and upper bounds of Young's modulus, respectively.

4.2. SKO method for bars structures

The SKO method has been used to obtain the optimal design of linear bars structures [13]. Using this method, once the maximum stress and reference stress of bars are obtained after finite element analysis, the temperature index of each bar is calculated by Eqs.(8)-(10) [9, 13]. The temperature index has no definite physical meaning, which is an intermediate variable bridging the stress to the Young's modulus.

$$T_j^{(k)} = T_j^{(k-1)} - s_j^{(k)}(\sigma_j^{(k-1)} - \sigma_{ref(j)}^{(k)}) \tag{8}$$

$$T_j^{(k-1)} = \begin{cases} 100 & T_j^{(k-1)} \ge 100 \\ 0 & T_j^{(k-1)} \le 0 \\ T_j^{(k-1)} & \text{otherwise} \end{cases} \tag{9}$$

$$s_j^{(k)} = T_0 / \sigma_{ref(j)}^{(k)} \tag{10}$$

where $\sigma_j^{(k\text{-}1)}$ is the maximum stress of member j in the (k-1)-th iteration, and $\sigma_{ref(j)}^{(k)}$ is the reference stress of member j in the k-th iteration. The reference stress equals either the average stress of all bars or the average stress of member j and its adjacent bars in a design domain. In general, the optimization process convergences faster by using the latter one as the reference stress, which is thus applied in this paper. $s_j^{(k)}$ is the step factor of member j in the k-th iteration. $T_j^{(k)}$ denotes the temperature index of member j in the k-th iteration, which has a linear relationship with the Young's modulus. $T_j^{(0)} = 0$ and $T_0 = 100$. According to Eqs.(8)-(10), if $\sigma_j^{(k\text{-}1)}$ is higher than $\sigma_{ref(j)}^{(k)}$, the temperature index of member j will be reduced and its Young's modulus will be increased; otherwise, the Young's modulus of member j will be reduced. When $T_j^{(k-1)} \le 0$, $E = E_{\max}$ is the real material Young's modulus. When $T_j^{(k-1)} \ge 100$, $E{=}E_{\min}{=}E_{\max}/1000$ [9].

4.3. Proposed Stability-Ensured Soft Kill Option (SSKO) algorithm

This paper proposes a novel SSKO algorithm based on the SKO method for bars structures and stability indices. The SSKO algorithm is divided into three stages: initial analysis, preliminary optimization, and stability-ensured optimization, shown in Fig.2. Superior to other algorithms, SSKO detects the buckling chord members through MSI and subsequently freezes them and their relative web members during the stability-ensured optimization stage. The relative bracing system [17] is the most common bracing system applied in large scale three-dimensional frame structures, especially in boom structures. Fig.3 shows the initial structure of a typical standard section of boom structures, which is composed of chord members and web members. The exterior web members are located at the six outer surfaces of a standard section, and the other web members are interior web members. In order to reinforce the buckling chord members identified though MSI, we present a technique of “freeze”, which means that Young's modulus is set to the true value of the real material and cannot be modified. When a chord member is judged to be buckling we will first freeze itself and its exterior relative members (Fig.4(a)), then in the following iteration if the chord member is judged to be buckling again we will freeze its interior relative members (Fig.4(b)). A growth factor of the reference stress is introduced as a step function with respect to the iteration number to optimize the structure to have a volume close to the predefined target. All details will be explained in the following.

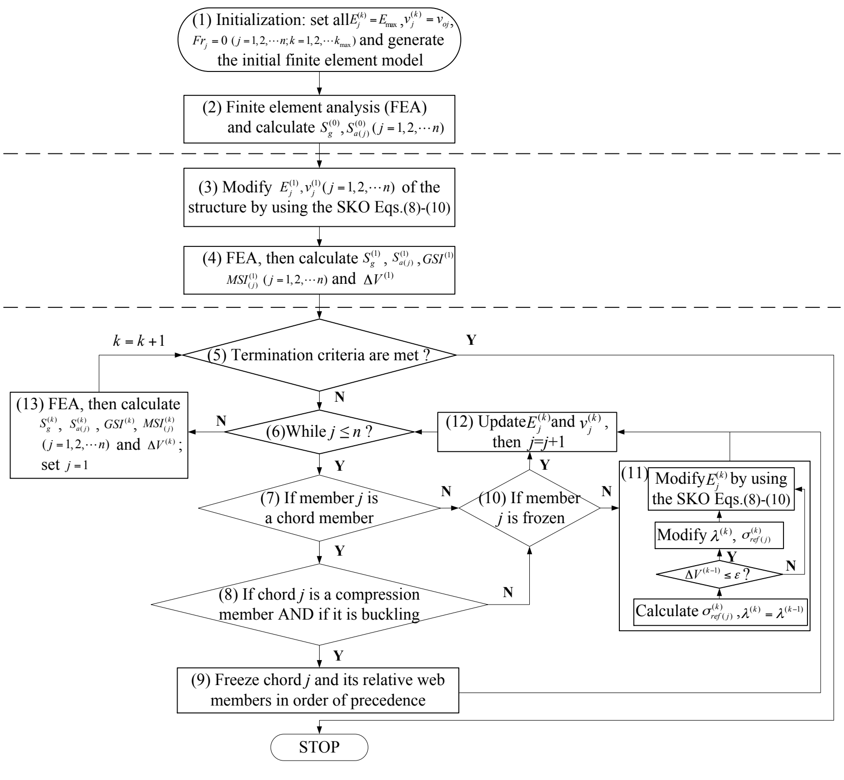

Figure 2: Flow chart of the SSKO algorithm

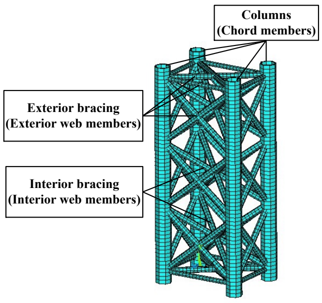

Figure 3: Initial structrue of a standard section

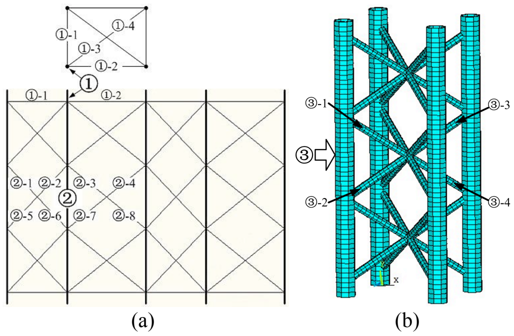

Figure 4: The relative members of a chord member

In the initial analysis stage (STEPs 1-2), this algorithm defines an initial finite element model and conducts geometrically nonlinear analysis, then calculates the overall stiffness $S_g^{(0)}$ and the axial stiffness of each compression member (Eq. (5)). $Fr_j = 0$ means that member *j* is not frozen, and $Fr_j = 1$ means member *j* is frozen. In the preliminary optimization stage (STEPs 3-4), the Young's modulus of each member is modified by the SKO Eqs. (8)-(10) directly, then the finite element analysis of the structure is carried out. Afterwards, the overall stiffness, the axial stiffness of compression members, GSI, MSI and the total volume change are calculated as the references of subsequent iterations. The stability-ensured optimization stage (STEPs 5-13) is the key part.

STEP 5: If any of the following criteria (Eqs. (11)-(14)) is met, stop the procedure. Otherwise, move to STEP 6.

$$\Delta V^{(k-1)} = \left|V^{(k-1)} - V^{(k-2)}\right| \le \varepsilon \text{ and } \Delta V^{(k-2)} = \left|V^{(k-2)} - V^{(k-3)}\right| \le \varepsilon \tag{11}$$

$$vf^{(k-1)} \le vf_{\text{target}} \text{ and } \Delta V^{(k-1)} \le \varepsilon \tag{12}$$

$$\sigma_{\max}^{(k-1)} \ge [\sigma] \tag{13}$$

$$k > k_{\max} \tag{14}$$

In Eq. (11), the tolerance of total volume change ε is a sufficently small positive real number. The total volume change among the last three iterations should be lower than ε. The volume fraction in the last iteration reaches the target volume fraction and the total volume change in the last iteration is lower than the tolerance, as shown in Eq. (12). Generally, the total volume change is required to be equal to zero in order to get a topology with the steady distribution of Young's modulus. The maximum stress in the last iteration is greater than the allowable stress (Eq. (13)). The maximum iteration number $k_{\max}$ is a sufficently large positive integer. If the iteration number *k* becomes larger than $k_{\max}$, the procedure terminates.

STEP 6-STEP12: Check all members in a design domain one by one, and update the Young's modulus of each member. STEP 8 is to judge whether chord *j* is buckling by Eq. (6), and STEP 9 is to freeze chord *j* and its relative web members. If member *j* is not frozen, its Young's modulus can be modified by the SKO Eqs. (8)-(10). The reference stress $\sigma_{ref(j)}^{(k)}$ in the SKO equations should be raised by Eqs. (15)-(17) to make the structure to be close to the target volume fraction if the total volume change in the last iteration is lower than ε.

$$\sigma_{ref(j)}^{(k)} = \sigma_{ref(j)}^{(k)} \lambda^{(k)} \tag{15}$$

$$\lambda^{(k)} = \lambda^{(k-1)} + \Delta\lambda^{(k)} \tag{16}$$

$$\Delta\lambda^{(k)} = \frac{1 - vf^{(k-1)}}{1 - vf_{\text{target}}} \Delta\lambda_{\max} \tag{17}$$

Here, $\lambda^{(k)}$ denotes the growth factor of the reference stress, and $\lambda^{(0)} = 1$. $\Delta\lambda^{(k)}$ means the increment of the growth fact, and $\Delta\lambda_{\max}$ is the maximum increment of the growth fact in each iteration, such as $\Delta\lambda_{\max} = 0.15$. When the volume fraction of the structure becomes closer to the target volume fraction, the increment of the growth factor gets larger.

The modified reference stress may be larger than the allowable stress sometimes, so this procedure records the original reference stress $\sigma_{ref}^{origin} = \sigma_{ref(j)}^{(k)}$, then adjusts the reference stress and the growth factor by Eqs. (18)-(19).

$$\sigma_{ref(j)}^{(k)} = [\sigma] \tag{18}$$

$$\lambda^{(k)} = [\sigma] / \sigma_{ref}^{origin} \tag{19}$$

STEP 13: Execute FEA, then calculate $S_g^{(k)}$, $S_{a(j)}^{(k)}$, $GSI^{(k)}$, $MSI_{(j)}^{(k)}$ $(j = 1, 2, \quad n)$ and $\Delta V^{(k)}$. Reset $j = 1$, go back to STEP 5.

5. An illustrative example

A 45.5m-long combined boom of 2500-tonne ring crane (see Fig.5) is studied as an illustrative example. All the twelve standard sections are replaced by typical standard sections (Fig.3 and Fig.6). Considering the symmetry of the combined boom, only half structure is analyzed. Fig.7 shows the finite element model of the half-boom. The left part of Fig.7 is the view of the luffing plane (XY plane), and the right part is the view of the swing plane (YZ plane). The range of the boom is 10m ("range" refers to the horizontal distance between the center of boom foot pins and boom tip pins), a lifting load F_Q=14320000N is applied at the lifting point, and a +X direction wind load F_W=26778N is uniformly distributed on end points of chord members of standard sections.

To improve the calculation efficiency, the plate structures at the ends of the boom are simplified as rigid bars, which belong to non-design domain. At the top of boom, only the Z-axis rotational and Y-axis translational degrees of freedom are released. At the bottom of boom, only the Z-axis rotational degree of freedom is released. At the symmetry plane of the whole combined boom, the Z-axis translational degree of freedom is constrained.

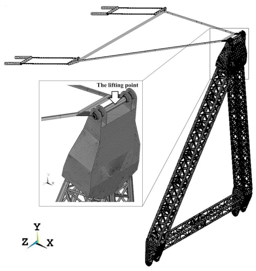

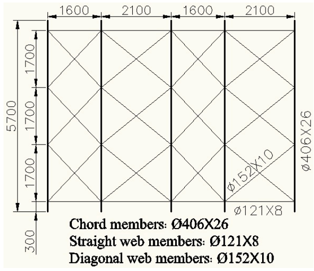

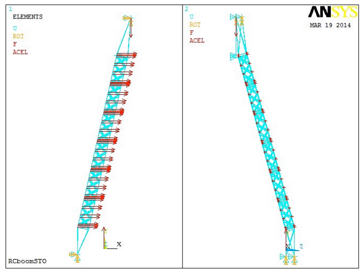

Figure 5: A 45.5m boom structure Figure 6: Dimensions of standard section Figure 7: FE model of half-boom

Three scenarios are applied in the topology optimization of this boom structure, and their performances are listed in Table 2. We make $\Delta\lambda_{\max}$ equal a large number in scenario 2-1, intentionally to get a fast convergence speed, but it turns out not to be the case. Fig.8 is the optimization results using scenario 2-1 (The layout of Fig.8(a) and Fig.9 is the same as Fig.7). It is obvious that this topology is not the optimal solution because the stress of most retained members is lower than 380MPa and the maximum stress which is above 500MPa happens at a local connection area (see Fig.8(a)). Fig.8(b) shows that the maximum stress begins to fluctuate divergently from the 40th iteration and goes beyond the allowable stress in the 141st iteration resulting in termination of optimization process. The GSI decreases to a minimum of 0.5465 in the 139th iteration but the structure still keeps in a stable state. The volume fraction also begins to fluctuate divergently from the 40th iteration as a result of the growth factor of the reference stress λ exceeding 2.5. When the growth factor becomes large, the reference stress gets an enormous growth at each step that leads to a sharp decrease of the volume fraction (Eq. (8)). It means that a considerable portion of material is removed which usually causes the occurrence of stress concentration (see Fig.8(a)). The maximum stresses of many members become higher than the reference stress in the subsequent iterations, so the volume fraction increases after its significant decrease. It has also been demonstrated by other case studies we conducted that under most circumstances λ should not be larger than 2.5 in order to ensure the stability of optimization.

Table 1: The performances of SSKO algorithm in boom structure problem

Scenario	vf_{target}	$\Delta\lambda_{\max}$	$[\sigma]$	GSI	Volume fraction	Max. stress	No. of Iterations
2-1	0.5	0.90	500	0.8969	0.8163	571.14	141
2-2	0.5	0.30	500	0.9860	0.7823	173.68	84
2-3	0.5	0.15	500	0.9860	0.7823	173.68	129

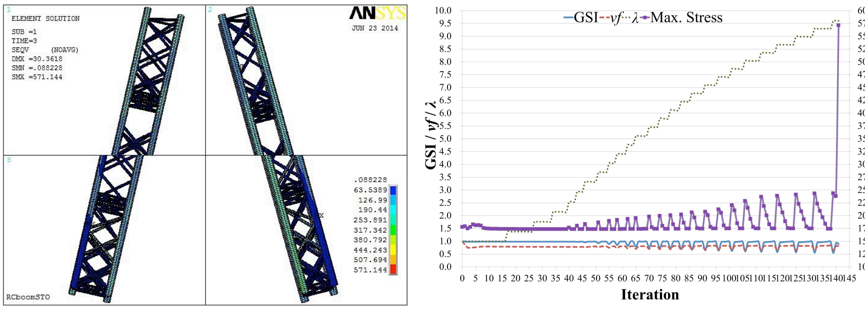

(a) (b)

Figure 8: Optimization results by scenario 2-1 (a) von Mises stress (b) Convergence history

The maximum increment of the growth factor is reduced in scenarios 2-2 and 2-3 to make the optimization process more stable. The optimization results (see Fig.9) are the same by either scenario 2-2 or 2-3, which justifies the proposed SSKO algorithm. Fig.10 shows the convergence histories of the SSKO algorithm in boom structure problem by strategies 2-2 and 2-3 respectively. The procedures converge after several step growths of λ, and the scenario 2-2 has a higher optimization efficiency than the scenario 2-3. The anti-buckling mechanism works well since the GSI keeps at around 1. The volume fraction decreases to 0.7823 and the maximum stress becomes 173.68MPa eventually.

(a) (b)

Figure 9: Optimization results by either scenario 2-2 or 2-3 (a) von Mises stress (b) displacement

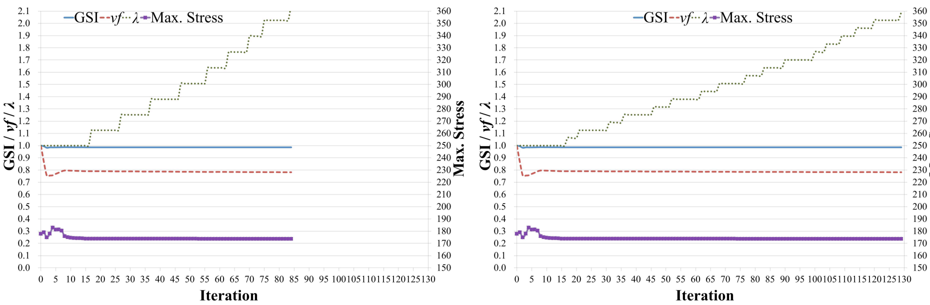

(a) (b)

Figure 10: Convergence histories of SSKO algorithm by scenarios (a)2-2 (b)2-3, respectively

The SSKO algorithm reduces the total volume significantly and gives a stable optimal design with the maximum stress being lower than the predetermined stress limit as long as we select an appropriate maximum increment of the growth factor. This example also demonstrates the high efficiency since it convergences to the same result through only a few dozens of iterations.

6. Conclusions

This paper presents a Stability-Ensured Soft Kill Option (SSKO) algorithm for structural topology design of geometrically nonlinear boom structures including stress constraints. This algorithm is developed for bars structures with large number of constraints by employing the proposed global stability index (GSI), compression member stability index (MSI) and the knowledge of bracing systems for resisting buckling of columns. The MSI can be used to distinguish the buckling of almost any kinds of compression members in boom structures. The results of the boom structure problem indicates that an appropriate maximum increment of the growth factor plays a crucial role in converging to the optimal design. The consistent optimization results using different scenarios demonstrate the applicability of the SSKO algorithm. The proposed algorithm can be applied to optimize other boom structures with different layout of web members as long as we develop a proper freezing strategy for the specific initial structure.

7. Acknowledgements

Funding for this research was provided by the National Natural Science Foundation of China (NSFC) under award number 51375345. Financial support for the first author, Wenjun Li, was provided in part by the China Scholarship Council.

8. References

[1] O. Makoto and I. Kiyohiro, *Stability and optimization of structures generalized sensitivity analysis*, Springer, New York, 2007.

[2] D. Manickarajah, Y. M. Xie and G. P. Steven, Optimisation of columns and frames against buckling, *Computers & Structures*, 75(1), 45-54, 2000.

[3] R. Kemmler, A. Lipka and E. Ramm, Large deformations and stability in topology optimization, *Structural and Multidisciplinary Optimization*, 30(6), 459-476, 2005.

[4] E. Lund, Buckling topology optimization of laminated multi-material composite shell structures, *Composite Structures*, 91(2), 158-167, 2009.

[5] E. Lindgaard and E. Lund, Nonlinear buckling optimization of composite structures, *Computer Methods in Applied Mechanics and Engineering*, 199(37-40), 2319-2330, 2010.

[6] E. Lindgaard and E. Lund, A unified approach to nonlinear buckling optimization of composite structures, *Computers & Structures*, 89(3-4), 357-370, 2011.

[7] E. Lindgaard and J. Dahl, On compliance and buckling objective functions in topology optimization of snap-through problems, *Structural and Multidisciplinary Optimization*, 47(3), 409-421, 2013.

[8] O. Sigmund and K. Maute, Topology optimization approaches A comparative review, *Structural and Multidisciplinary Optimization*, 48(6), 1031-1055, 2013.

[9] A. Baumgartner, L. Harzhem and C. Mattheck, SKO (Soft Kill Option) - The biological way to find an optimum structure topology, *International Journal of Fatigue*, 14(6), 387-393, 1992.

[10] C. Mattheck, *Design in nature: learning from trees*, Springer-Verlag, Berlin, New York, 1998.

[11] L. Harzheim and G. Graf, A review of optimization of cast parts using topology optimization - I - Topology optimization without manufacturing constraints, *Structural and Multidisciplinary Optimization*, 30(6), 491-497, 2005.

[12] L. Harzheim and G. Graf, A review of optimization of cast parts using topology optimization - II - Topology optimization with manufacturing constraints, *Structural and Multidisciplinary Optimization*, 31(5), 388-399, 2006.

[13] W. Li, Q. Zhou, X. Zhang et al., Topology optimization design of bars structure based on SKO method, *Applied Mechanics and Materials*, 394(1), 515-520, 2013.

[14] Z. Shen, C. Su and Y. Luo, Application of Strut Model on Steel Spatial Structure, *Building Structure*, 37(1), 8-11, 2007. [In Chinese]

[15] F. Fan, J. Yan and Z. Cao, Stability of reticulated shells considering member buckling, *Journal of Constructional Steel Research*, 77, 32-42, 2012.

[16] C. Y. Lin and F. M. Sheu, Adaptive volume constraint algorithm for stress limit-based topology optimization, *Computer-Aided Design*, 41(9), 685-694, 2009.

[17] American Institute of Steel Construction (AISC), *Specification for Structural Steel Buildings* ANSI/AISC 360-10, Chicago, AISC, 2010.